Supporting Information

Syntheses, structures and catalytic properties of Evans−Showell-type Polyoxometalates-based 3D metal–organic complexes constructed from semi-rigid bis(pyridylformyl)piperazine ligand and transition metals

Feng-Cai Li*, Li-Kun Tan, Xi-Li Li, Hua-Jie Kong, Li-Ming Ge, Ling-Yu Yue and Li-Feng Han

Henan Provincial Key Laboratory of Surface and Interface Science, Zhengzhou University of Light Industry, Zhengzhou, 450002, PR China

CONTENTS:

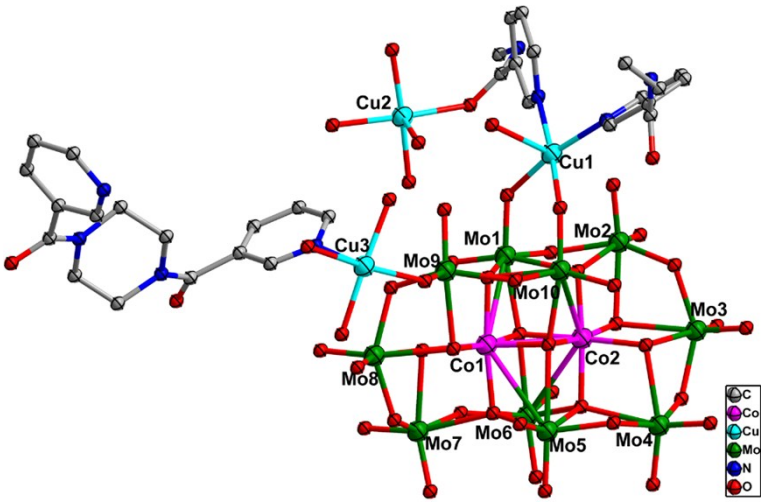

Fig. S1 ORTEP drawing of the asymmetric unit of compound **1** with thermal ellipsoids at 50% probability. Free water molecules are omitted for clarity.

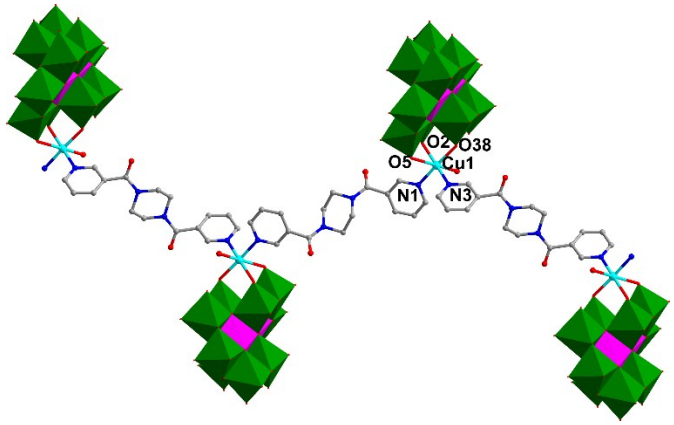

Fig. S2 The 1D infinite chain structure constructed from $\{Cu[Co_2Mo_{10}H_4O_{38}]\}$ units and L ligands in **1**.

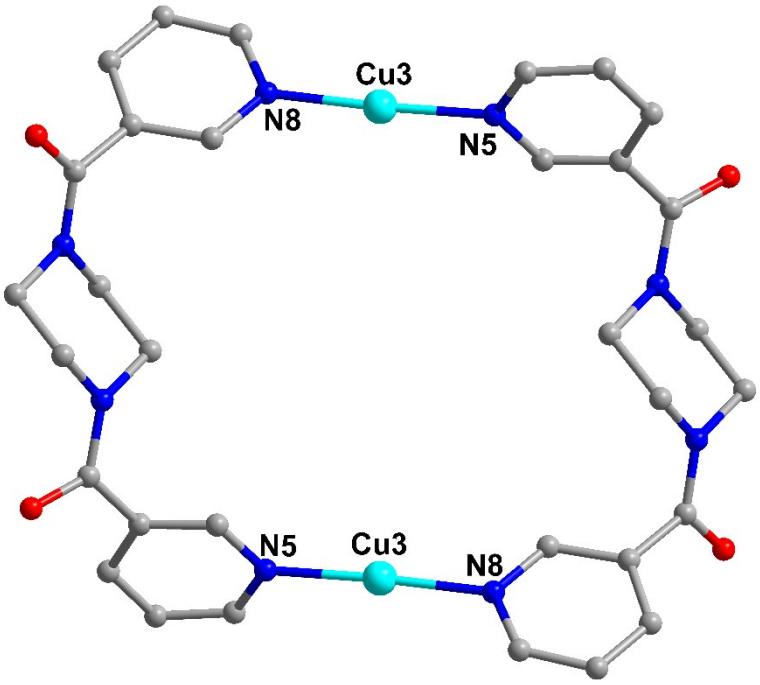

Fig. S3 The quadrate Cu_2L_2 loop constructed from Cu3 ions and L ligands in **1**.

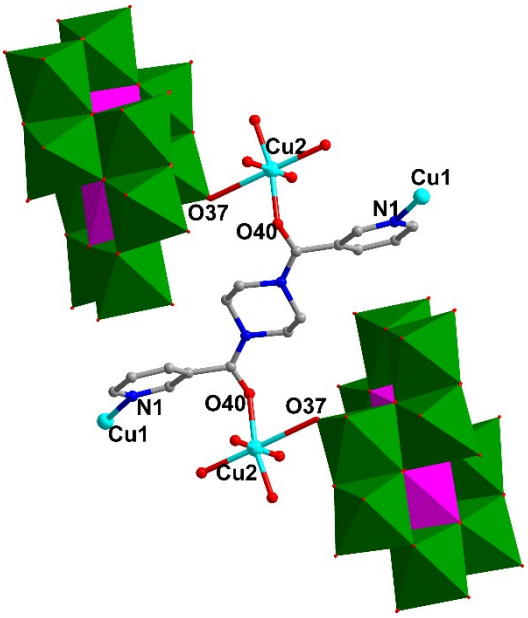

Fig. S4 The double {Cu[$Co_2Mo_{10}H_4O_{38}$]−L−Cu[$Co_2Mo_{10}H_4O_{38}$]} structure constructed from Cu2 ions and L ligands in **1**.

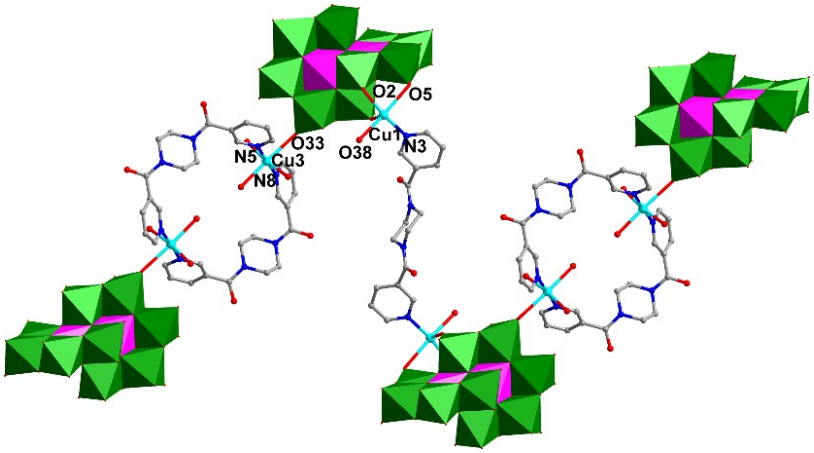

Fig. S5 The 1D Zigzag chain structure constructed from {Cu[$Co_2Mo_{10}H_4O_{38}$]−L−Cu[$Co_2Mo_{10}H_4O_{38}$]} units and the Cu_2L_2 loops in **1**.

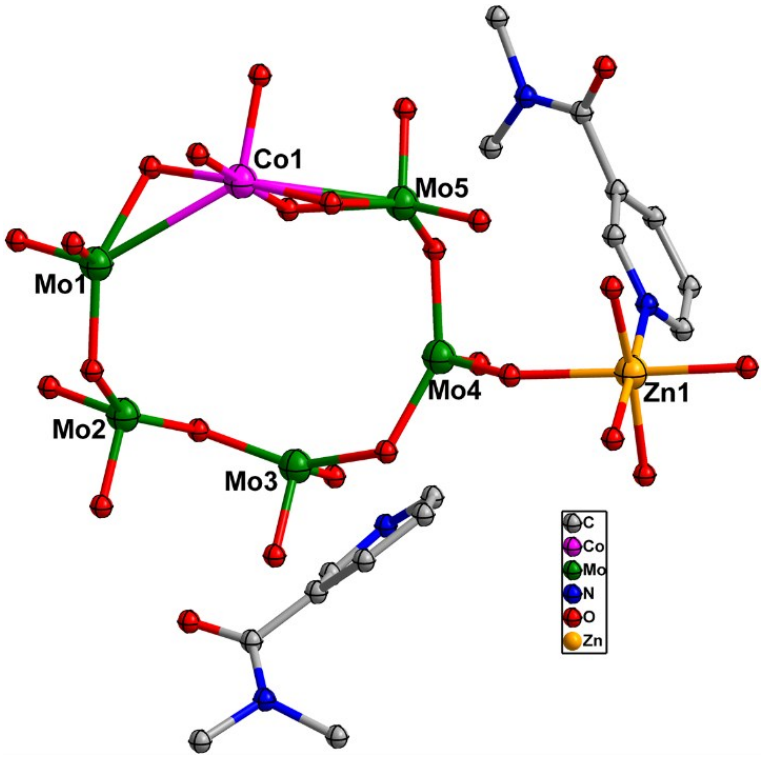

Fig. S6 ORTEP drawing of the asymmetric unit of compound **2** with thermal ellipsoids at 50% probability. Free water molecules are omitted for clarity.

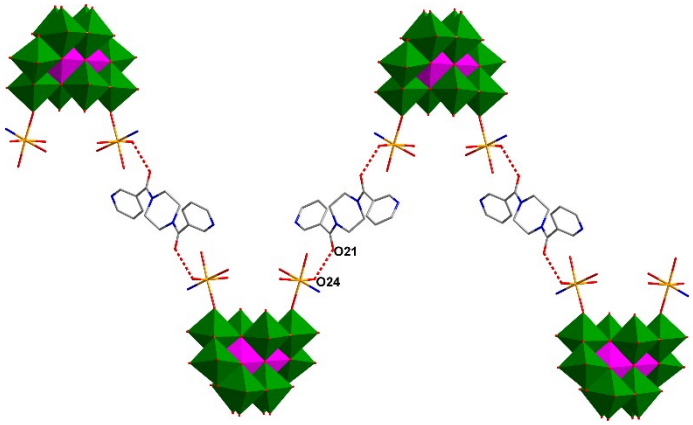

Fig. S7 A view of the 1D chain between $\{Zn(H_2O)_4[Co_2Mo_{10}H_4O_{38}]\}$ units and the protonated H_2L ligands formed through the hydrogen bonding interaction [O24-H24B···O21] in **2**.

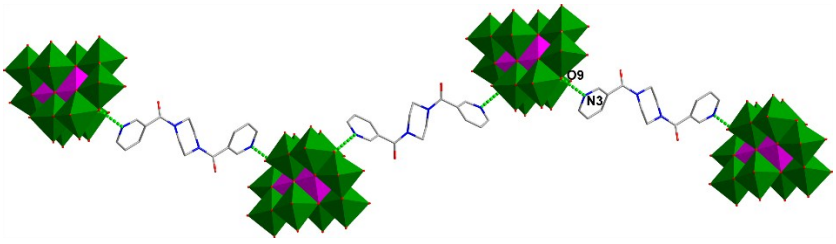

Fig. S8 A view of the 1D chain between $[Co_2Mo_{10}H_4O_{38}]$ anions and the protonated H_2L ligand formed through the hydrogen bonding interaction [N3-H3···O9] in **2**.

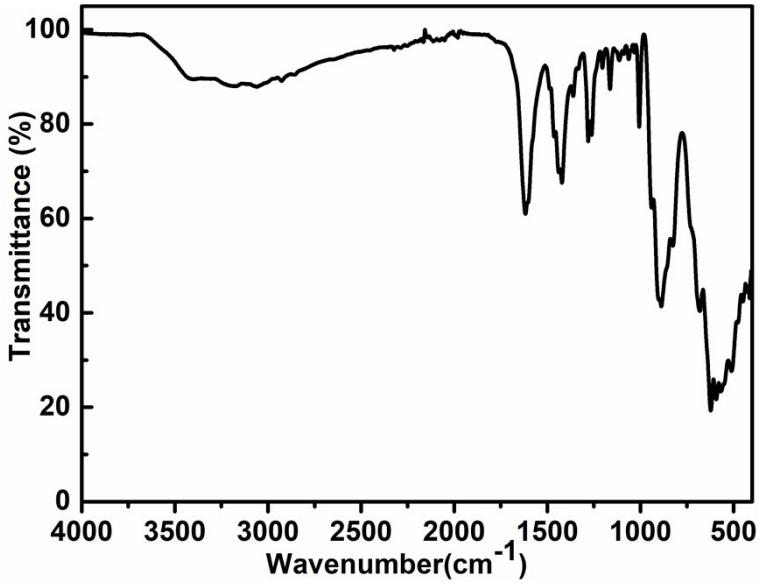

Fig. S9 IR spectrum for compound **1**.

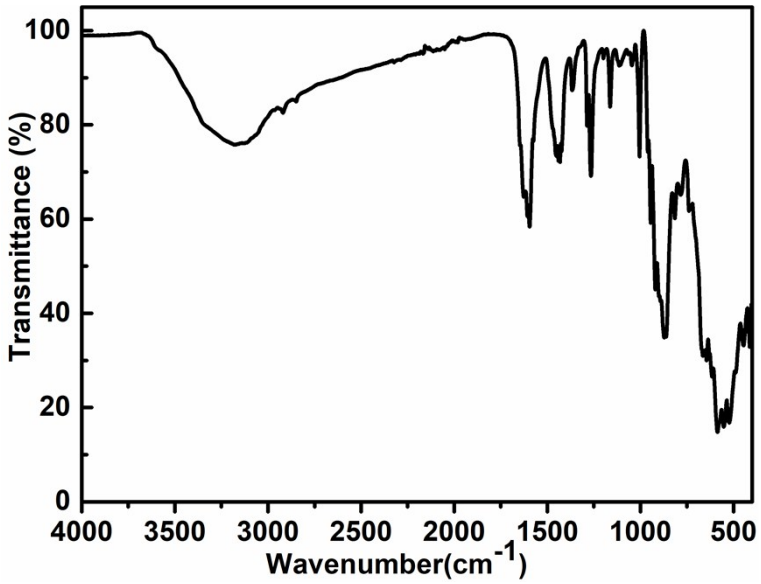

Fig. S10 IR spectrum for compound **2**.

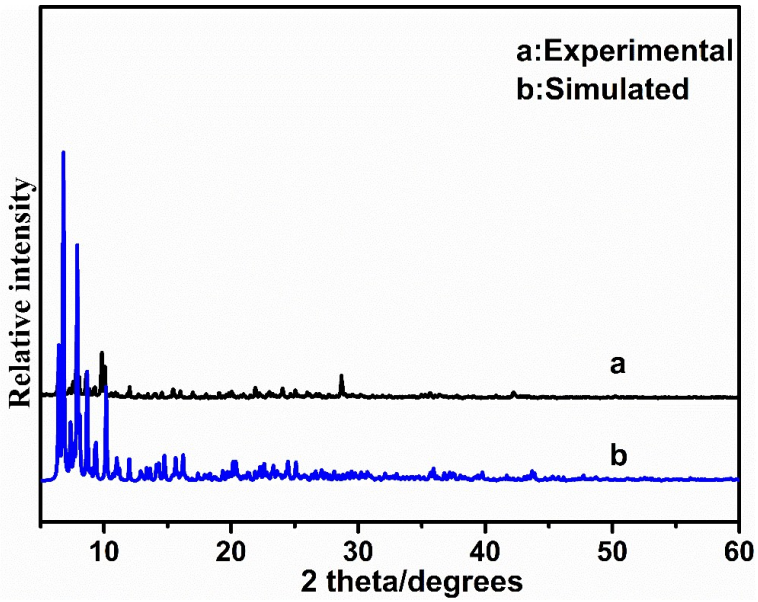

Fig. S11 The Simulated and experimental PXRD patterns for compound **1**.

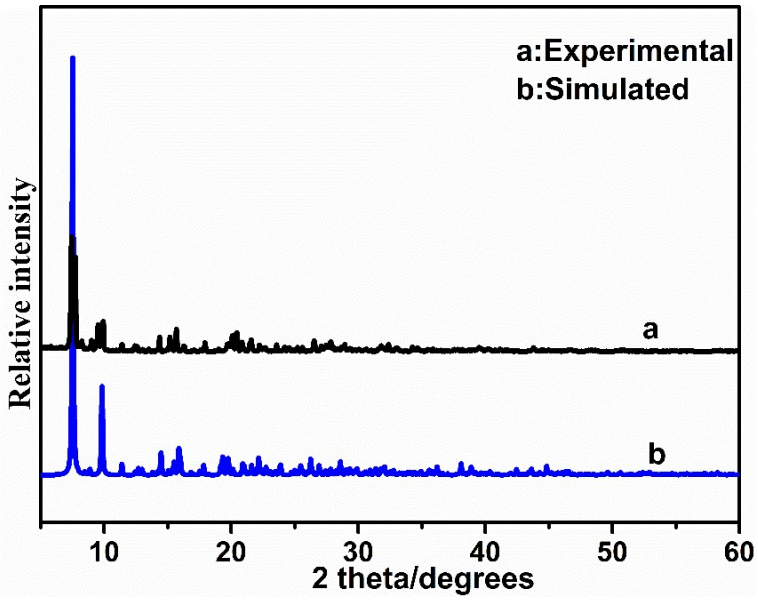

Fig. S12 The Simulated and experimental PXRD patterns for compound **2**.

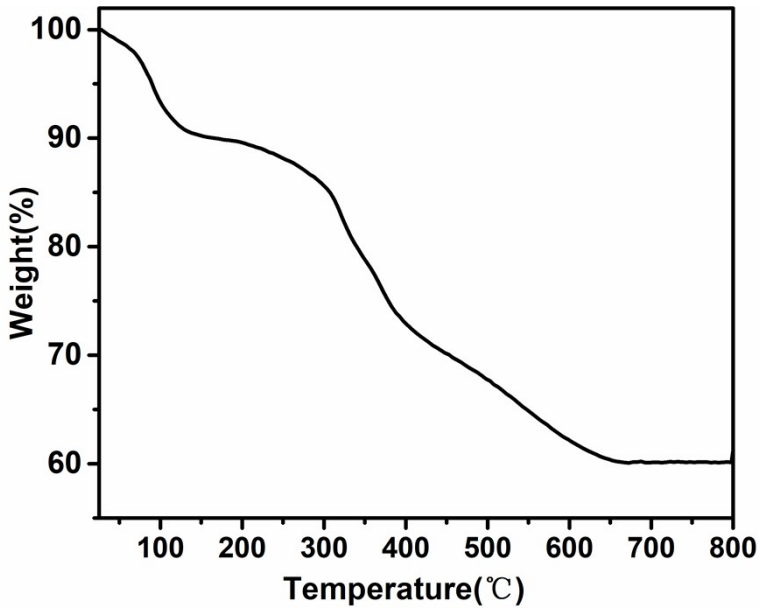

Fig. S13 TG curve for compound **1**.

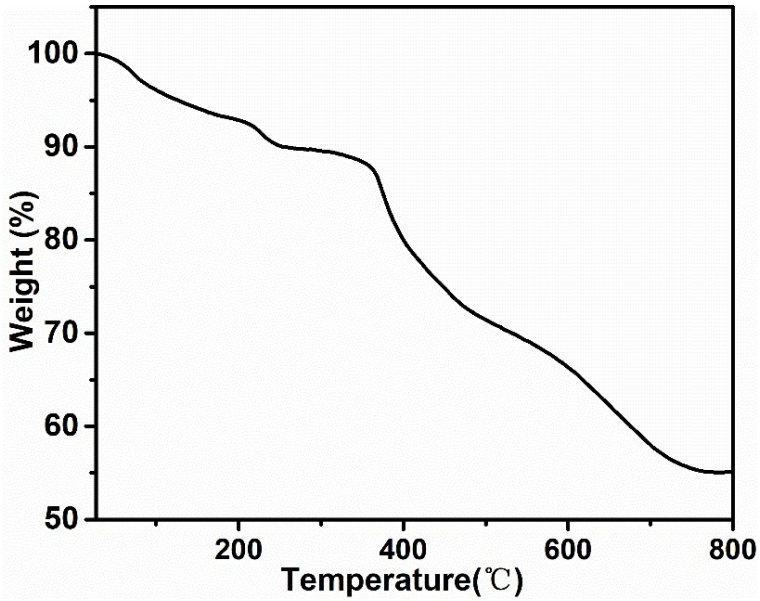

Fig. S14 TG curve for compound **2**.

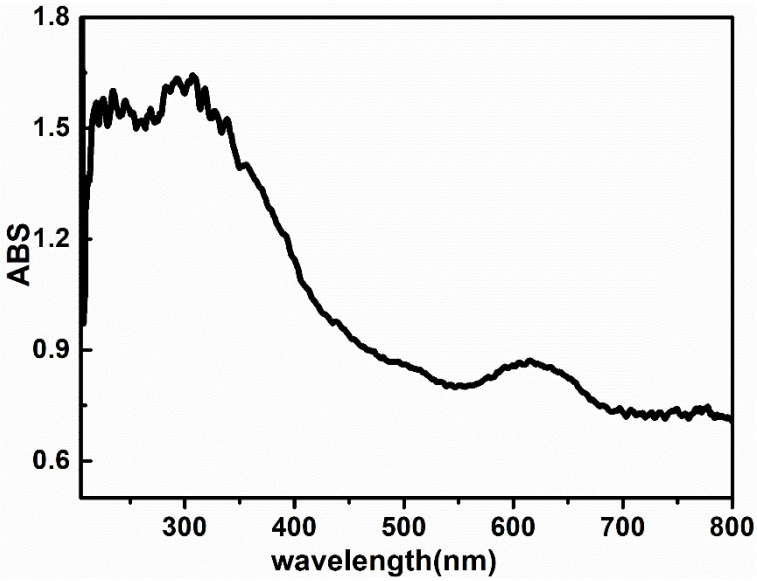

Fig. S15 UV−vis absorption spectrum of solid state compound **1**.

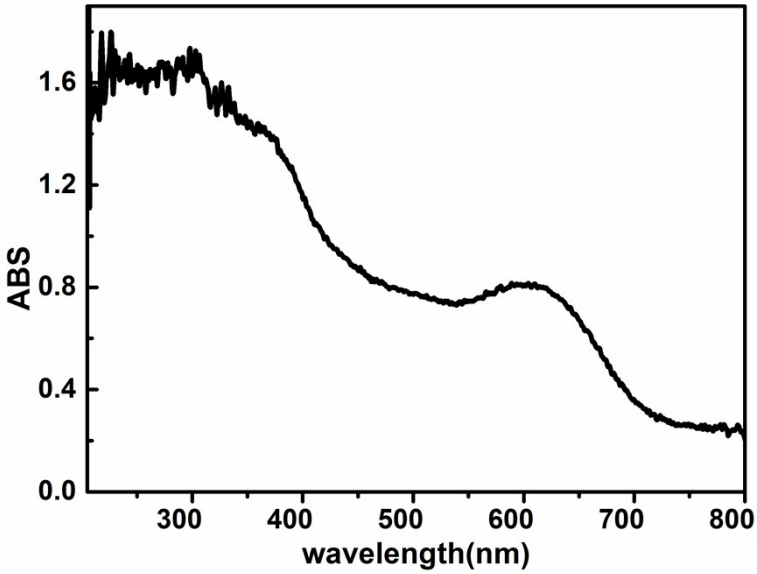

Fig. S16 UV−vis absorption spectrum of solid state compound **2**.

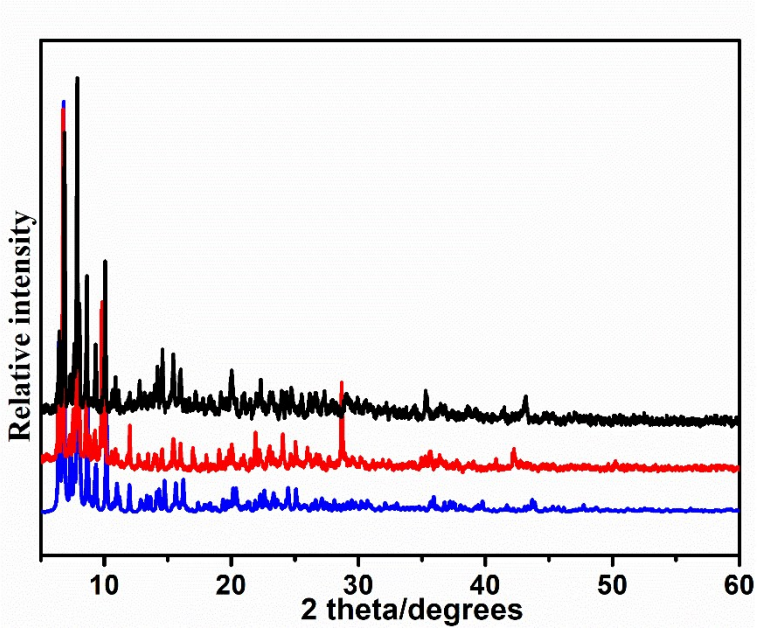

Fig. S17 Powder X-ray diffraction (PXRD) patterns of **1**: calculated pattern from crystal data (blue line); experimental pattern before catalysis (red line); recovered catalyst **1** after three catalytic runs of Oxidation of benzyl alcohol (black line).

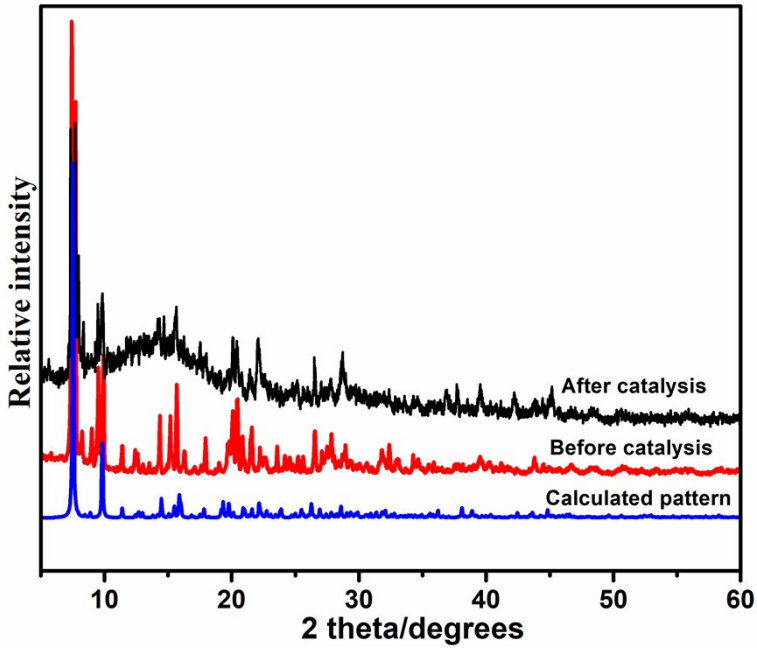

Fig. S18 Powder X-ray diffraction (PXRD) patterns of **2**: calculated pattern from crystal data (blue line); experimental pattern before catalysis (red line); recovered catalyst **2** after 1 catalytic runs of Oxidation of benzyl alcohol (black line).

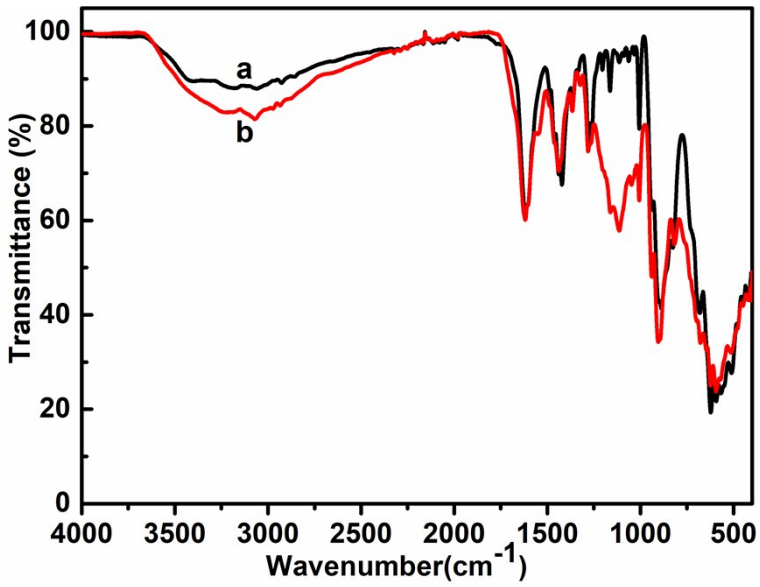

Fig. S19 IR spectrum for (a) as-synthesized compound **1** and (b) recovered catalyst after catalysis reaction.

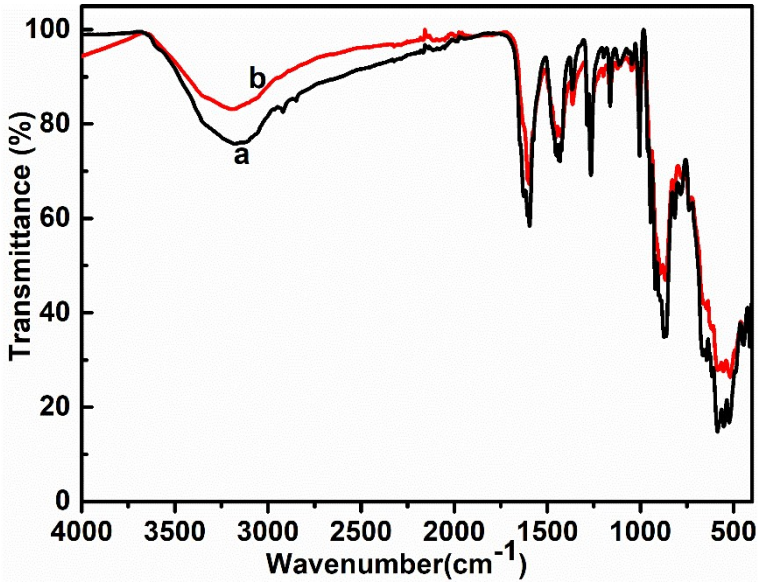

Fig. S20 IR spectrum for (a) as-synthesized compound **2** and (b) recovered catalyst after catalysis reaction.

Table.S1 Selected bond distances (Å) and angles (°) for the title complexes.

	Complexe 1		
	Bond distances (Å)		
Cu1–N1	2.017(11)	Cu2–O45	1.972(17)
Cu1–N3	1.999(11)	Cu2–O46	1.963(18)
Cu1–O50	2.325(13)	Cu3–N5	2.019(12)
Cu1–O2	1.988(10)	Cu3–N8[3]	2.012(13)
Cu1–O38	1.986(9)	Cu3–O47	1.977(12)
Cu1–O5	2.592(11)	Cu3–O33	2.478 (11)
Cu2–O40	2.028(14)	Cu3–O48	1.994(10)

Cu2–O37[4]	2.577(10)	Cu3–O49	2.316(12)
Cu2–O43	1.951(15)	Cu3[3]– N8	2.012(13)
Cu2–O44	2.225(18)		
	Bond angles (°)		
N1–Cu1–O50	87.5(5)	O37–Cu2–O45	88.6(5)
N3–Cu1–N1	92.7(5)	O37–Cu2–O46	84.6(6)
N3–Cu1–O50	95.4(5)	O45–Cu2–O40	167.4(7)
O2–Cu1–N1	91.5(4)	O45–Cu2–O44	91.4(7)
O2–Cu1–N3	169.4(5)	O46–Cu2–O40	94.9(7)
O2–Cu1–O50	94.5(4)	O46–Cu2–O44	93.4(8)
O38–Cu1–N1	174.6(5)	O46–Cu2–O45	85.8(8)
O38–Cu1–N3	88.3(4)	N5–Cu3–O49	88.6(5)
O38–Cu1–O50	87.0(4)	N8[3]–Cu3–N5	177.2(5)
O38–Cu1–O2	88.4(4)	N8[3]–Cu3–O49	94.2(5)
O5–Cu1–N1	89.1(3)	O33–Cu3–N5	89.9(4)
O5–Cu1–O2	81.8(4)	O33–Cu3–N8	87.2(4)
O5–Cu1–O50	174.9(4)	O33–Cu3–O47	84.2(4)
O5–Cu1–O38	96.2(3)	O33–Cu3–O48	88.4(3)
O5–Cu1–N3	88.4(4)	O33–Cu3–O49	175.9(3)
O40–Cu2–O44	101.1(6)	O47–Cu3–N5	87.6(5)
O43–Cu2–O40	86.3(6)	O47–Cu3–N8[3]	92.1(5)
O43–Cu2–O44	91.1(7)	O47–Cu3–O48	172.0(5)
O43–Cu2–O45	91.9(7)	O47–Cu3–O49	91.9(5)
O43–Cu2–O46	175.0(8)	O48–Cu3–N5	89.0(5)
O37–Cu2–O40	78.9(4)	O48–Cu3–N8[3]	90.9(4)
O37–Cu2–O43	90.8(5)	O48–Cu3–O49	95.2(4)
O37–Cu2–O44	178.0(5)		
Symmetry codes for **1**: [1]-X,1-Y,2-Z; [2]2-X,-Y,2-Z; [3]2-X,-Y,1-Z; [4]-1+X, Y, Z			
	Complexe 2		
	Bond distances (Å)		
Zn1–N1	2.085(13)	Zn1–O23	2.140(19)
Zn1–O11	2.210(11)	Zn1–O24	2.010(12)
Zn1–O22	2.024(14)	Zn1–O25	2.121(19)
	Bond angles (°)		
N1–Zn1–O11	87.2(5)	O24–Zn1– N1	99.5(6)
N1–Zn1–O23	177.9(6)	O24–Zn1–O11	89.5(5)
N1–Zn1–O25	93.7(6)	O24–Zn1–O22	163.4(7)
O22–Zn1–N1	97.1(6)	O24–Zn1–O23	82.3(7)
O22–Zn1–O11	90.4(5)	O24–Zn1–O25	92.2(6)
O22–Zn1–O23	81.1(7)	O25–Zn1– O11	177.9(6)
O22–Zn1–O25	87.7(6)	O25–Zn1–O23	87.3(7)
O23–Zn1–O11	91.7(6)		
Symmetry codes for **2**: [1]1-X,1-Y,1-Z; [2]1-X,+Y,1/2-Z; [3]3/2-X,1/2-Y,-Z			

Table S2. Selected hydrogen–bonding geometry (Å, °) for complex 2

D–H···A	D–H	H···A	D···A	<(DHA)
O22-H22B...O13	0.90	1.77	2.641(17)	161.3
O24-H24A...O5_$1	0.90	2.11	2.845(17)	137.9
O24-H24B...O21_$1	0.90	1.82	2.704(16)	168.8
N3-H3...O9	0.86	1.83	2.649(16)	157.5
$1:1.5-X,-0.5+Y,0.5-Z				

Table S3. Reutilization data for oxidation of benzyl alcohol to benzaldehyde benzoic acid ($PhCO_2H$) over catalyst **1** and **2**.

Catalyst	Conv. (%) at 10 h	Product sele.(%) $PhCO_2H$ at 10 h
1		
Round 1	99.4	98.8
Round 2	98.9	97.1
Round 3	98.2	95.8
2		
Round 1	85.0	59.8
Round 2	76.2	58.4
Round 3	68.0	54.2

Table S4. Catalytic Results for **1** Tested in Liquid-Phase Oxidation of Benzyl Alcohol under different catalytic conditions.

Catalyst	Substrate	Factors	Conversion (%)	product selectivity (%)	
				PhCHO	$PhCO_2H$
		Time (h)[a]			
1	BzOH	6	86.0	21.8	78.2
1	BzOH	8	98.3	4.0	96.0
1	BzOH	10	99.4	1.2	98.8
1	BzOH	12	99.6	0.8	99.2
		Temperature(℃)[b]			
1	BzOH	50	70.3	54.8	45.2
1	BzOH	75	99.4	1.2	98.8
1	BzOH	100	100	–	100%
		Amount of oxidant TBHP [c]			
1	BzOH	1.5 equiv	96.9	6.1	93.9
1	BzOH	3 equiv	99.4	1.2	98.8
1	BzOH	4.5 equiv	99.3	0.7	99.3
		Amount of Catalyst [d]			
1	BzOH	0.75 mol%	99.1	2.9	97.1

1	BzOH	1.5 mol %	99.4	1.2	98.8
1	BzOH	3.0 mol %	98.7	2.6	97.4

[a] Reaction conditions: alcohol (0.25 mmol, 1 equiv), catalyst **1** (3.75 μmol, 1.5 mol%), TBHP (3 equiv), acetonitrile (1 mL), 75℃, N_2, different time.

[b] Reaction conditions: alcohol (0.25 mmol, 1 equiv), catalyst **1** (3.75 μmol, 1.5 mol%), TBHP (3 equiv), acetonitrile (1 mL), different temperature(℃) , N_2, for 10 h.

[c] Reaction conditions: alcohol (0.25 mmol, 1 equiv), catalyst **1** (3.75 μmol, 1.5 mol%), TBHP (1.5 equiv; 3 equiv; 4.5 equiv), acetonitrile (1 mL),75℃, N_2, for 10 h.

[d] Reaction conditions: alcohol (0.25 mmol, 1 equiv), catalyst **1**(1.875μmol, 0.75 mol% ; 3.75 μmol, 1.5 mol%; 7.5 μmol, 3.0 mol%), TBHP (3 equiv), acetonitrile (1 mL), 75℃, N_2, for 10 h.

Table S5. Catalytic Results for **2** Tested in Liquid-Phase Oxidation of Benzyl Alcohol under different duration of catalytic reaction.

Catalyst	Substrate	Time (h)[a]	Conversion (%)	product selectivity (%)	
				PhCHO	$PhCO_2H$
2	BzOH	6	57.5	70.4	29.6
2	BzOH	8	66.2	58.4	41.6
2	BzOH	10	85.0	40.2	59.8
2	BzOH	12	86.5	35.4	64.6

[a] Reaction conditions: alcohol (0.25 mmol, 1 equiv), catalyst **2** (3.75 μmol, 1.5 mol%), TBHP (3 equiv), acetonitrile (1 mL), 75℃, N_2, different time.

Table S6. Literature Data for Molybdenum–Copper Catalysts and Molybdenum–Zinc Catalysts Tested in the Liquid Phase Oxidation of Benzyl Alcohol.

catalyst	Solvent/T (°C)/ oxidant	time (h)	oxidant /BzOH/ cat.	Conv. (%)	Product sele.(%)		reaction system	Ref
					PhCHO	$PhCO_2H$		
$\{Cu_3(L_1)_{1.5}(H_2O)_5[Co_2Mo_{10}H_4O_{38}]\}\cdot 5H_2O$ (L_1 = N,N′-bis(2-pyrazinecarboxamide)-1,4- butane)	CH_3CN /75/ TBHP	10	1:3:1.5mol %	93.4	19.6	80.4	heterogeneous	28
$\{[Cu(L_2)_{0.5}(H_2O)_2]_2[Co_2Mo_{10}H_4O_{38}]\}\cdot 6H_2O$ (L_2 = N,N′-bis(2-pyrazinecarboxamide)-1,6-hexane)	CH_3CN /75/ TBHP	10	1:3:1.5mol %	100	2.1	98.0	heterogeneous	28
$(en)[Cu_3(ptz)_4(H_2O)_4]$ $[Co_2Mo_{10}H_4O_{38}]$	CH_3CN /75/ TBHP	8/24	1:3:1.5mol %	59.7/98.7	100/0	0/92	heterogeneous	27
$[Cu_4(\mu_4\text{-}O)(tr_2ad)_2(MoO_4)_3]$	TFT/75/ TBHP	1/4/24	153:100:1 (based on Mo)	1/17/85	100/100/26	0/0/70	heterogeneous	37
$[Cu_4(\mu_4\text{-}O)(tr_2ad)_2(MoO_4)_3]$	TFT/75/ TBHP	1/4/24	113:75:1 (based on Cu)	18/53/88	100/45/28	0/54/66	heterogeneous	37
$[Cu_2(tr_2ad)_4](Mo_8O_{26})$	TFT/75/TBHP	1/4/24	153:100:1(based on Mo)	10/55/81	100/49/25	0/41/65	heterogeneous	37
$[Cu_2(tr_2ad)_4](Mo_8O_{26})$	Tol/75/ TBHP	1/4/24	153:100:1(based on Mo)	10/55/81	100/49/25	0/41/65	heterogeneous	37
$MoO_2(acac)_2$ and $Cu(NO_3)_2$	Tol/100/ O_2	3	1 atm/20:1:1	100	98	/	homogeneous	59
$(NH_4)_6[Mn(H_2O)_2Mo_8O_{28})]$	Tol/80/H_2O_2	8	2.15g:0.43g:0.02g	72.3	100	/	homogeneous	36
α-$[Cu(mIM)_4]V_2O_6$	C_6H_5Cl /120/H_2O_2	8	4:1:4.1%	98.5	100	/	heterogeneous	34

$[HMTAH]_2[\{Zn(H_2O)_5\}\{Zn(H_2O)_4\}\{Mo_7O_{24}\}]\cdot 2H_2O$	Solvent free/80/H_2O_2	9	180:20:1	50%	100	/	heterogeneous	35